RASĀYAN *J. Chem.*
Vol. 17 | No. 2 |567-575| April - June | 2024
ISSN: 0974-1496 | e-ISSN: 0976-0083 | CODEN: RJCABP
http://www.rasayanjournal.com
http://www.rasayanjournal.co.in

SYNTHESIS AND CHARACTERIZATION OF PANI–La_2O_3 BINARY NANOCOMPOSITE FOR ELECTRODE MATERIAL IN SUPERCAPACITOR

Kusum Lata, Jyoti Redhu and Ravi Kumar Rana✉
Department of Chemistry, Baba Mastnath University, Asthal Bohar, Rohtak-124021, India
✉Corresponding Author: hit.ravirana@gmail.com

ABSTRACT

We report the preparation of polyaniline (PANI) covered La_2O_3 binary composite material using in situ oxidative-polymerization method using APS as oxidant in acidic medium. Prepared material was characterized using X-ray diffraction (XRD) and Fourier transform infrared spectroscopy (FTIR) to understand the structure and bonding. Transmission electron microscopy (TEM) estimated the particle size confirming the synthesis of particles in nanorange. For chemical composition and thermal stability, energy dispersive X-ray and thermogravimetric (TG) analysis respectively were performed. Cyclic voltametric measurement of PANI-La_2O_3 nanocomposite having a semi–rectangular loop of high area exhibited high specific conductance (Csp = 373 Fg−1). The high ionic and electrical conductivity alongwith high charge storage capability makes PANI-La_2O_3 nanocomposite a potential candidate for its usage as electrode material in supercapacitor.

Keywords: Polyaniline; nanocomposite; thermal stability; conductance; supercapacitor.
RASĀYAN *J. Chem.*, Vol. 17, No.2, 2024

INTRODUCTION

The advancement in the materials have always shaped human culture and contributed significantly to the growth of human civilizations. The understanding of the effect of the materials structure at the micro and nano sizes opened a large study arena, where the nanocomposites are occupying a remarkable space.[1,2] A family of materials known as nanomaterials have diameters in the nanometer range, generally between 1 and 100 nm. A new class of materials known as nanocomposites has been created when these nanomaterials are combined in a continuous material phase to create a composite while maintaining their physical identities both before and after.[3,4] Comparing this novel category of materials to their components in their uncombined forms reveals that nanocomposites possess superior qualities with improved hardness, mechanical strength, high electrical and thermal conductivity, low friction, strong corrosion and wear resistance etc.[5,6] The high surface to volume ratio of nanoparticles is a significant characteristic which determines the usefulness and distinctive features of material.[7] Additionally, the quantity and kind of flaws in smaller–sized components are reduced as a result of the differences in characteristics between nanomaterials and their respective bulk equivalents.[8]

Because of their low costs, simple preparation, modest density, good ecological stability and high mechanical strength, conducting polymers (CPs) have become very popular as electrodes for supercapacitors.[9,10] CPs combine the desirable properties corresponding to traditional polymers with unique electronic characteristics when compared to metals or semiconductors.[11,12] Due to its distinct redox states and strong theoretical capacitance properties, PANI is one amongst the most attractive electrodes among CPs.[13–15] However, the electrochemistry is complicated because there are at least two redox processes and three significant oxidation states. It is important to keep in mind that the extent of protonation and oxidation states have a significant impact on the conductive properties of PANI. Conductive PANI is only synthesised by doping half-oxidized states using protonic or functionalized acids, whereas fully reduced states and fully oxidised states are not always conducting.[16] Although employing PANI as the electrodes for supercapacitors has numerous potential benefits, the actual applications are currently constrained by a number of drawbacks.[17,18] As anions or cations are doped or undoped into CP during repeatedly occurring charging and discharging steps, associated volumetric changes, including swelling, breaking, or shrinking in the skeleton, can lead to mechanical breakdown

http://doi.org/10.31788/RJC.2024.1728773

and break the chains.[19] For this reason, PANI electrodes demonstrate little cycle stability, which is inevitable. Second, in processes with recurring cycles, the associated reduction in electrical conductivity causes the specific capacitance to degrade quickly, leading to a relatively low-rate capability.[20] Thirdly, because reactions do not spread into the bulk of the material in practise and only a few nanometres of PANI materials from the surface layer are used in the redox reactions, the innermost part of the electrodes is unable to be completely utilised, resulting in a much smaller experimental specific capacitance than the value predicted.[21] In addition, the specific capacitance and cycle stability are significantly impacted by the loss caused by PANI peeled off from the active materials.[22] Two efficient methods should be used to enhance the electrochemical functionality of PANI electrodes. The logical construction of nanostructured electrodes is one potential alternative. If the size shrinks to the nanoscale, new reactions will take place in the inner layer of the active substances, resulting in decreased ion or electron transport routes in addition to high utilisation efficiency. Another well-known strategy is to provide a superior mechanical matrix to stop PANI materials from being structurally ground up.[23] A possible method for enhancing PANI performance is the creation of nanocomposites of PANI and inorganic nanoparticles, with the goal of creating materials that exhibit a synergetic or supportive response of PANI and inorganic nanomaterials.[24–26]

In light of the above, we describe an electrode material La_2O_3 embedded in a PANI matrix, resulting in a La_2O_3/PANI composite. X-ray diffraction (XRD), FTIR and transmission electron microscopy were used to analyse structure, crystallinity and particle size of composite. Using cyclic voltammetry and electrochemical impedance spectroscopy, the electrochemical characteristics were assessed.

EXPERIMENTAL

Preparation of polyaniline

The chemical oxidative polymerization technique was used to prepare Polyaniline (PANI) by with the help of aniline monomer. In this polymerisation process, hydrochloric acid is used as catalyst and ammonium peroxide–sulfate as an oxidizing agent. Initially, 5 g aniline monomer was dissolved in distilled water (200 ml) in a volumetric flask followed by addition of HCl dropwise to maintain a pH ~1. Ammonium peroxide–sulfate i.e., $(NH_4)_2S_2O_8$ (6.125 g) was dissolved in distilled water (100 ml) in another volumetric flask. Furthermore, the two solutions were mixed, by adding the second solution in aniline solution dropwise for about 30 min stirred for three hours to mix homogeneously. Then it was kept at RT for 24 h for polymerisation to take place.[27] The green precipitates of PANI formed were washed HCl and acetone. PANI formed as emeraldine salt left for drying in air and afterwards it was dried in vacuum ~ 70 °C (3 h).[28,29]

Preparation of La_2O_3

La_2O_3 nanoparticles are formed at a lower temperature using a combustion method. Water is utilised as a solvent, while $La(NO_3)_3.6H_2O$ and urea are employed as source materials. To create a homogeneous aqueous solution, the estimated quantity of lanthanum nitrate was dissolved into a 100 ml beaker. This solution was then heated at 80 °C. Free water is evaporated during heating, creating a gel-like substance. A measured quantity of urea was then added, along with some distilled water, and a paste was produced before being heated. The purpose of the urea that was added was to dissolve the metal ions evenly in the reaction solution by forming complexes with them. For around 15 minutes, the paste was heated to 500 °C in a furnace. During the process of heating the material, which produced the product, there was water evaporation, decomposition and gas evolution.

Preparation of PANI-La_2O_3 nanocomposite

The ultrasonication method was used to create the binary PANI-La_2O_3 nanocomposite. A similar quantity of PANI and La_2O_3 was introduced to 100 ml of deionized water and held there for 90 minutes of ultrasonication. Finally, the solution was washed, dried at 70 °C, and crushed into powder.[30]

Detection Method

The crystalline structure and phase composition of the sample were investigated by recoding the diffraction pattern of samples using Rigaku Ultima-IV diffractometer with Bragg-Brentano geometry

using CuKα radiation having wavelength of 1.5416 A°. X-ray pattern of the materials was recorded from 15°–70° (2 Theta angle) having scanning speed of 2°/minute and 0.02° step interval. The IR spectral profile was recorded using an FTIR spectrometer (PerkinElmer 5700) using KBr as a reference. The morphology and average particle size of the samples was determined by using TECNAI (200 kV) transmission electron microscope (TEM). Elemental analysis and chemical composition of PANI-La_2O_3 composite was executed on Ametek (energy dispersive X-ray spectrometer). At a heating rate of 10 °C min-1, prepared samples' thermograms (30-1000 °C) were recorded using a Hitachi STA 7300 thermogravimetric analyser. Ivium potentiostat was used to understand the redox behavior of composite material.

RESULTS AND DISCUSSION

X-ray diffraction study

Using diffraction analysis, the crystal structure and phase of the prepared samples were determined. The XRD patterns of pure La_2O_3 and a PANI-La_2O_3 nanocomposite are shown in Fig.-1. The synthesis of highly crystalline materials is indicated by the presence of strong diffraction peaks in the XRD profiles. Diffraction pattern of La_2O_3 was found to be closely related to the hexagonal structure and P63/mmc (194) space group of La_2O_3 with JCPDS 83-1355.[31] Additionally, the lack of foreign peaks in the La_2O_3 diffraction pattern demonstrated the very pure synthesis of the material under consideration. Additionally, a nearly identical diffraction pattern showing no appreciable peak deviations from La_2O_3 was seen for the PANI-La_2O_3 composite material, revealing the homogenous participation of both PANI and La_2O_3 phases in the nanocomposite. The optimal interaction between the various phases in the nanocomposite is demonstrated by a minor change in a few peak positions.[32]

With the help of Scherrer's formula (Equation 1), the crystal size was calculated from FWHM of the strongest peak. The determined crystal size for La_2O_3 and PANI-La_2O_3 was found to be 42.02 and 41.36 nm respectively.

$$D = k\lambda/(\beta.\cos\theta) \quad (1)$$

D = average crystallite size, k = constant, X-ray wavelength (λ) = 0.15416 nm, θ = angle of diffraction, β = full width at half maxima (FWHM).

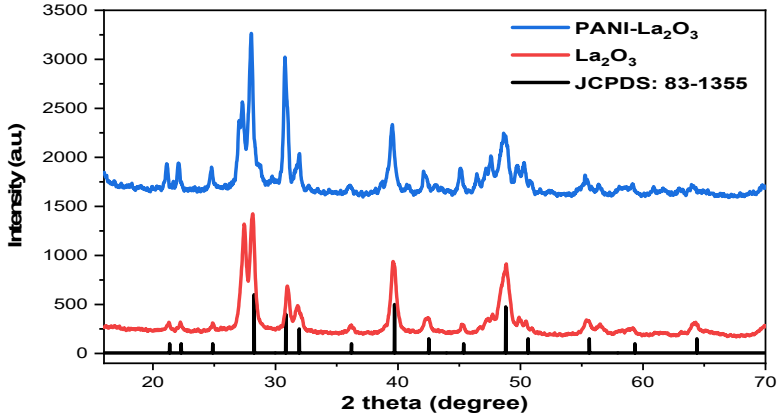

Fig.-1: Diffraction patterns of La_2O_3 and PANI-La_2O_3 matched with JCPDS

Table-1: Various diffraction parameters of La_2O_3 and PANI-La_2O_3 samples

Sample	Area	Width	FWHM (□)	Particle size (nm)
La_2O_3	1199.984	1.039	1.224	42.02
PANI-La_2O_3	1279.822	1.120	1.319	41.36

FTIR study

FTIR spectrum PANI-La_2O_3 binary composite was recorded to analyse its structural and bonding characteristics. The spectrum was obtained in the 400–4000 cm^{-1} range as shown in Fig.-2. The spectrum of composite material contains a peak at 836 cm^{-1} corresponding to C–H out of plane bending on the 1, 4 positions of the aromatic ring of PANI. The characteristic peaks at 1170 and 1310 have been assigned to C–N=C and C–N–C aromatic bonds of PANI.[33] Spectrum also reveals bands at 1560 and 1406 cm^{-1} corresponding to C–C stretching of quinoid and benzenoid rings in PANI. C–N and C=N stretching

appears at 1278 cm^{-1} in the FTIR spectrum.[34] The occurrence of the benzenoid and quinoid units is the indication of the conductive emeraldine form of PANI. Broad band situated at 3407 cm^{-1} has been assigned to N–H stretching vibration of PANI.[27,35] The characteristic peaks corresponding to La–O vibrations were observed at 546, 615, 728 cm^{-1}.

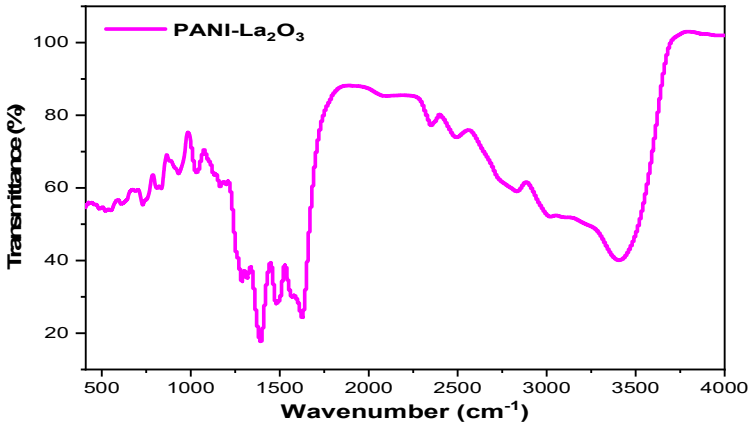

Fig.-2: FTIR spectrum of PANI-La_2O_3 binary composite material

TEM investigation

TEM was employed to examine the dimensions and shape of developed composite material. The nearly spherical PANI-La_2O_3 particles are seen in the TEM picture along with some aggregation (Fig.-3). The material exhibits a consistent distribution of particles with a size between 45 and 70 nm. The slightly uneven distribution of mass and heat throughout the synthetic process is what causes the somewhat irregular shape and varied sizes of the particles. This composite material may be useful as supercapacitor electrodes because of the production of nanoparticles.

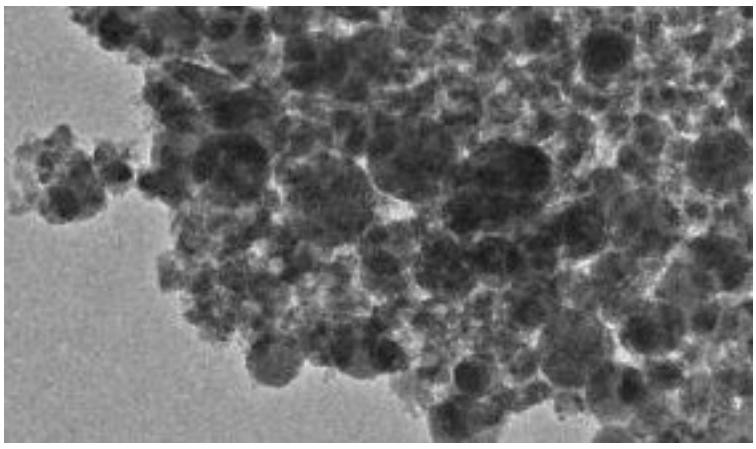

Fig.-3: TEM image of PANI-La_2O_3 binary nanocomposite.

EDX analysis

EDX analysis was done to verify the preparation of PANI-La_2O_3 nanocomposite. The matching peaks for the elements included in the sample were seen when various parts of the sample were focused, as shown in Fig.-4. Only the peaks in the spectrum that match La and O are present. The synthesis of pure PANI-La_2O_3 nanocomposite is confirmed by the lack of peaks that correspond to extraneous components other than the ingredients. Table-2 lists the information related to EDX spectrum of PANI-La_2O_3 in terms of atomic and weight percentages. A homogeneous formation of the material with a suitable elemental dispersion encouraging structural analyses was suggested by the existence of distinctive peaks in the spectrum.

TGA Analysis

To evaluate the thermal stability of the synthesized PANI-La_2O_3, thermo-gravimetric analysis was carried out. The progressive weight loss transition phases, which correspond to moisture loss and the breakdown

of organic matter, are revealed in temperatures range 30–900 °C in a N_2 environment. At a lower temperature, PANI-La_2O_3 starts to degrade (Fig.-5).

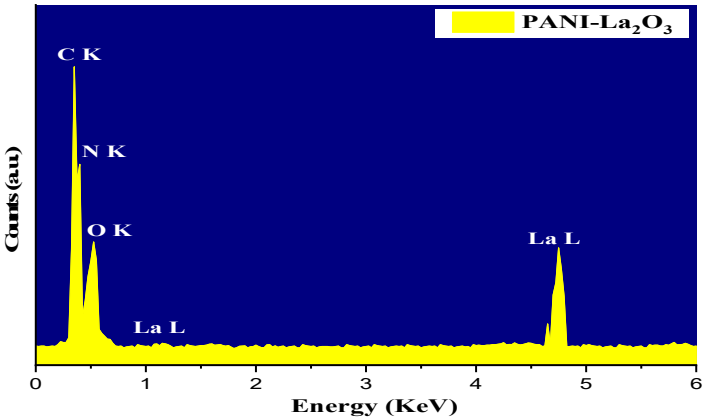

Fig.-4: EDX spectrum of PANI–La_2O_3 nanocomposite

Table-2: Chemical composition of PANI-La_2O_3 composite in atomic and weight percentage.

Element	Weight %	Atomic %
C K	38.16	54.89
N K	24.79	17.80
O K	20.72	15.86
La L	16.33	11.45

For composite, the first weight loss was noted at 41.19 °C, followed by weight loss of 5.81 % between 41.19 and 120 °C due to the elimination of H_2O molecules, weight loss of 39.64 % between 120 and 450 °C indicated the elimination of small-molecular-weight oligomers, and a decrease in weight of 82.69 % between 450 and 625 °C indicated the decomposition of the nanocomposite matrix. This behaviour could be the result of La_2O_3 particles acting as catalysts, which increase the temperature at which PANI degrades. The interaction between PANI and La_2O_3 is responsible for the PANI-La_2O_3 compound's excellent thermal stability.[36]

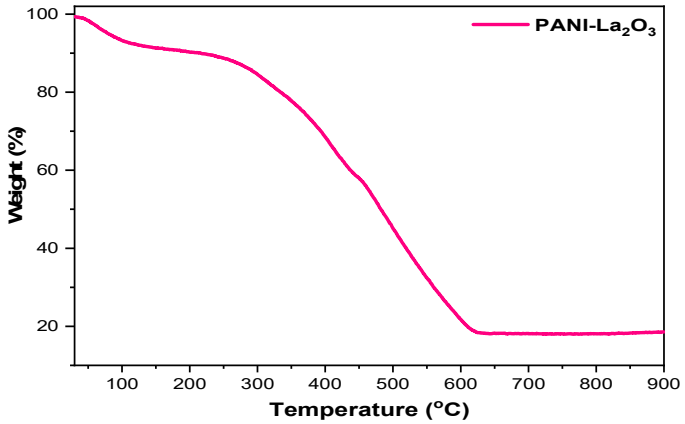

Fig.-5: Thermo-gravimetric curve of PANI-La_2O_3 nanomaterial

Current-voltage measurements (I–V)

The I–V characteristics of PANI-La_2O_3 binary composite have been depicted in Fig.-6. I–V plot of the considered nanocomposite exhibited outstanding ohmic character at room temperature. The high conductivity of the sample approved it as an excellent material for usage in electrode materials for supercapacitors.

Cyclic voltammetry (CV)

To study the electrochemical properties of the PANI-La_2O_3 composite, CV was carried out using a three-electrode cell construction in a 1 molar KOH electrolyte at a voltage (0–0.6 V). Figure-7 exhibits the

cyclic voltammogram of PANI-La_2O_3 nanocomposite having a semi–rectangular loop of higher area indicating its higher value of specific conductance (C_{sp} = 373 Fg^{-1}) calculated as follows:

$$C_{sp} = \int \frac{IdV}{smV}$$

Where ∫IdV = area under the CV curve, s = sweep rate (10 mV/s), V = voltage range and m = loaded mass. The inorganic-organic association in nanocomposites, which could potentially improve the redox performance of the constructed electrode, is responsible for a high C_{sp} value.[37]

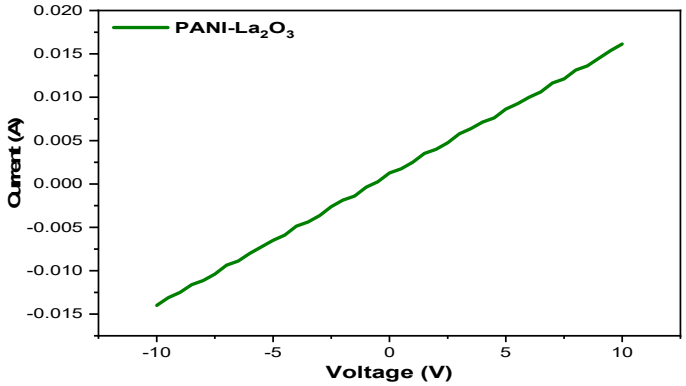

Fig.-6: I–V characteristics plot of PANI-La_2O_3 composite

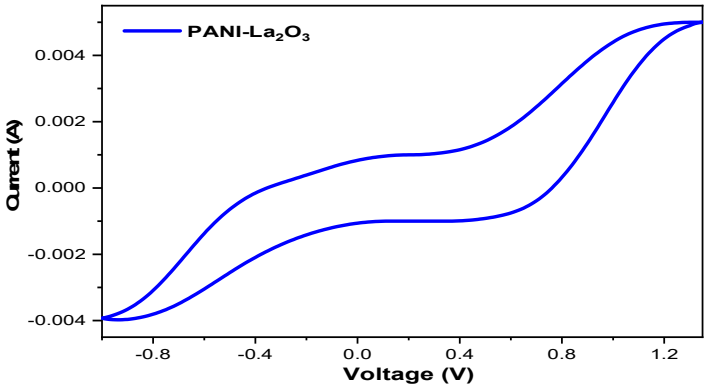

Fig.-7: Cyclic voltammogram of PANI-La_2O_3 binary composite

Electrochemical Impedance Spectroscopy (EIS)

The electrochemical behavior PANI-La_2O_3 binary composite of was further explored using EIS. The fitting of the analyzed data of all three electrode materials was done using Nyquist plots (Fig.-8) drawn between Z′ (actual part) and Z″ (imaginary portion) to attain net impedance (z). The linear and quasi-circular regions of Nyquist plot are located in low and high-frequency zone respectively. A compact semi-circle with a small diameter indicates a high level of ionic conductivity in PANI-La_2O_3 binary composite. I–V findings further supported the greater electrical conductivity. These findings indicate that the charge transfer rate is more important at the interface between the electrode and electrolyte surfaces, which therefore accounts for its high charge storage capability.[38]

CONCLUSION

PANI was prepared by technique. La_2O_3–PANI binary composite was synthesized by the in-situ chemical oxidative method. The prepared material was characterized using XRD, FTIR, TEM, EDX, TGA, cyclic voltammetry and EIS techniques to understand the composition, structural and electrochemical properties. Diffraction data confirmed the synthesis of uncovered and PANI-covered La_2O_3 having a hexagonal crystal structure and P63/mmc (194) space group. FTIR analysis supported XRD results exhibiting vibration bands corresponding to both PANI as well as La_2O_3.

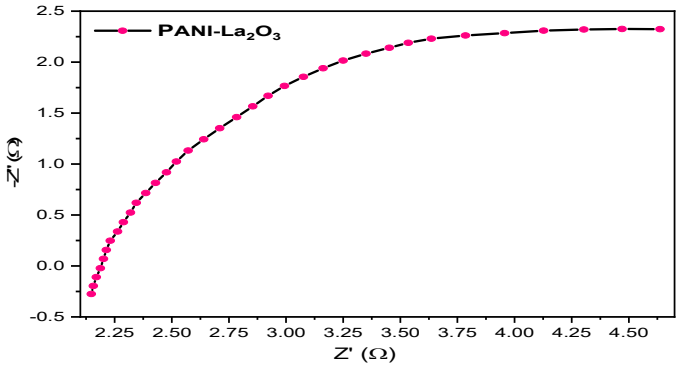

Fig.-8: Nyquist plot of PANI-La_2O_3 binary composite

TEM images revealed the formation of nanocomposite with some agglomeration. TG analysis exhibited the excellent thermal stability of the sample confirming the possible interaction between PANI and La_2O_3 in the composite. I–V and cyclic voltammetry revealed the high ionic and electrical conductivity along with high charge storage capability which were further supported by Nyquist plot of PANI-La_2O_3 nanocomposite. Due to such excellent electrochemical behavior, PANI-La_2O_3 binary composite could be used a potential candidate for its usage as electrode material in supercapacitors.

ACKNOWLEDGMENTS

No financial help has been received for this work.

CONFLICT OF INTERESTS

The authors declare that there is no conflict of interest.

AUTHOR CONTRIBUTIONS

All the authors contributed significantly to this manuscript, participated in reviewing/editing and approved the final draft for publication. The research profile of the authors can be verified from their ORCID ids, given below:

Kusum Lata http://orchid.org/0009-0008-1298-7881
Jyoti Redhu http://orchid.org/0009-0006-2814-5713
Ravi Kumar Rana http://orchid.org/0009-0004-4637-8401

REFERENCES

1. H. Kumar, A. Boora, A. Yadav, Rajni and Rahul, *Results in Chemistry*, **2**, 100046(2020), http://doi.org/10.1016/j.rechem.2020.100046
2. Z.A. Hu, Y.L. Xie, Y.X. Wang, L.P. Mo, Y.Y. Yang and Z.Y. Zhang, *Materials Chemistry and Physics*, **114**, 990(2009), http://doi.org/10.1016/j.matchemphys.2008.11.005
3. H. Kumar, M. Luthra, M. Punia and R.M. Singh, *Colloid and Interface Science Communications*, **45**, 100512(2021), http://doi.org/10.1016/j.colcom.2021.100512
4. H. Kumar, M. Luthra, M. Punia and D. Singh, *Colloids and Surfaces A: Physicochemical and Engineering Aspects*, **640**, 1(2022), http://doi.org/10.1016/j.colsurfa.2022.128464
5. N. Dong, M. Zhong, P. Fei, Z. Lei and B. Su, *Journal of Alloys and Compounds*, **660**, 382(2016), http://doi.org/10.1016/j.jallcom.2015.11.175
6. A.M. El-naggar, A. Alsaggaf, Z.K. Heiba, A.M. Kamal, A.M. Aldhafiri, A. Fatehmulla and M.B. Mohamed, *Optical Materials*, **139**, 113771(2023), http://doi.org/10.1016/j.optmat. 2023.113771
7. A. Yadav, H. Kumar, R. Sharma, R. Kumari and M. Thakur, *RSC Advances*, **12**, 24063 (2022), http://doi.org/10.1039/d2ra03554e

8. M. Alam, N.M. Alandis, A.A. Ansari and M.R. Shaik, *Journal of Nanomaterials*, **2013**, 157810(2013), http://doi.org/10.1155/2013/157810
9. M. Beygisangchin, S.A. Rashid, S. Shafie, A.R. Sadrolhosseini and H.N. Lim, *Polymers*, **13**, 2023(2021), http://doi.org/10.3390/polym13122003
10. S. Ishaq, M. Moussa, F. Kanwal, M. Ehsan, M. Saleem, T.N. Van and D. Losic, *Scientific Reports*, **9**, 5974 (2019), http://doi.org/10.1038/s41598-019-41939-y
11. J. Vivekanandan, V. Ponnusamy, A. Mahudeswaran and P.S. Vijayanand, *Applied Scientific Research*, **3**, 147(2011)
12. A. Yadav, H. Kumar, R. Sharma, R. Kumari, G. Kumar, A. Tundwal, A. Dhayal, A. Yadav and D. Singh, *Inorganic Chemistry Communications*, **158**, 111701(2023), http://doi.org/10.1016/j.inoche.2023. 111701
13. Z. Zeng, Y. Chen, X. Zhu and L. Yu, *Chinese Chemical Letters*, **34**, 107728(2023), http://doi.org/10.1016/j.cclet.2022.08.008
14. S.P. Ansari and F. Mohammad, *International Scholarly Research Notices*, **2012**, 129869(2012), http://doi.org/10.5402/2012/129869
15. V. Van Tran, T.T.V. Nu, H.R. Jung and M. Chang, *Polymers*, **13**, 3031 (2021), http://doi.org/10.3390/polym13183031
16. K. Namsheer and C.S. Rout, *RSC Advances*, **11**, 5659(2021), http://doi.org/10.1039/d0ra07800j
17. A. Varghese, K.R.S. Devi, S. Mathew, B. Saravanakumar and D. Pinheiro, *Materials Today: Proceedings*, (2023), http://doi.org/10.1016/j.matpr.2023.12.003
18. N. Sirotkin and A. Khlyustova, *Journal of Composites Science*, **7**, 174(2023), http://doi.org/10.3390/jcs 7040174
19. E.N. Zare, P. Makvandi, B. Ashtari, F. Rossi, A. Motahari and G. Perale, *Journal of Medicinal Chemistry*, 63, 1(2020), http://doi.org/10.1021/acs.jmedchem.9b00803
20. Q.M. Al-Bataineh, A.B. Migdadi, A. Telfah, A.A. Ahmad, A.M. Alsaad and C.J. Tavares, *Materials Chemistry and Physics*, **290**, 126387(2022), http://doi.org/.1016/j.matchemphys. 2022.126387
21. S.H. Kazemi, M.A. Kiani, R. Mohamadi and L. Eskandarian, *Bulletin of Materials Science*, **37**, 1001(2014), http://doi.org/10.1007/s12034-014-0037-y
22. P. Sengodu and A.D. Deshmukh, *RSC Advances*, **5**, 42109(2015), http://doi.org/10.1039/c4ra17254j
23. P. Singh and S.K. Shukla, *Surfaces and Interfaces*, **18**, 100410(2020), http://doi.org/10.1016/j.surfin.2019. 100410
24. P. Singh and S.K. Shukla, *Journal of Materials Science*, **55**, 1331 (2020), http://doi.org/10.1007/s10853-019-04141-z
25. S. Shahabuddin, N.M. Sarih, S. Mohamad and J.J. Ching, *Polymers*, **8**, 27(2016), http://doi.org/10.3390/polym 8020027
26. N. Jadhav, S. Kasisomayajula and V.J. Gelling, *Frontiers in Materials*, **7**,1(2020), http://doi.org/10.3389/fmats.2020.00095
27. U.S. Waware, G.J. Summers, A.M.S. Hamouda and M. Rashid, P*olymer-Plastics Technology and Engineering*, **57**, 1015(2018), http://doi.org/10.1080/03602559.2017.1370108
28. N.Y. Abu-Thabit, Journal of Chemical Education, **93**, 1606(2016), http://doi.org/10.1021/acs.jchemed. 6b00060
29. S.G. Dhole, S.A. Dake, T.A. Prajapati and S.N. Helambe, *Procedia Manufacturing*, **20**, 127(2018), http://doi.org/10.1016/j.promfg.2018.02.018
30. M.N. Ur Rehman, T. Munawar, M.S. Nadeem, F. Mukhtar, A. Maqbool, M. Riaz, S. Manzoor, M.N. Ashiq and F. Iqbal, *Ceramics International*, **47**,18497(2021), http://doi.org/10.1016/j.ceramint.2021.03.173
31. D. V. Dharmadhikari, S.K. Nikam and A.A. Athawale, *Journal of Alloys and Compounds*, **590**, 486(2014), http://doi.org/10.1016/j.jallcom.2013.12.141
32. R. Nekooie, T. Shamspur and A. Mostafavi, *Journal of Photochemistry and Photobiology A: Chemistry*, **407**, 113038(2021), http://doi.org/10.1016/j.jphotochem.2020.113038
33. Y.J. Prasutiyo, A. Manaf and M.A.E. Hafizah, *Journal of Physics: Conference Series*, **1442**, 012003(2020), http://doi.org/10.1088/1742-6596/1442/1/012003

34. P.L. Meena and J.K. Saini, *Results in Chemistry*, **5**, 100764(2023), http://doi.org/10.1016/j.rechem.2023. 100764
35. A. Senapati and A.K. Chakraborty, *Journal of Materials Science: Materials in Electronics*, **32**, 27794(2021), http://doi.org/10.1007/s10854-021-07161-1
36. A. Sharma, V. Kumar, S. Kumar, Pooja D, S. Bagchi and A.P. Bhondekar, *Advanced Materials Proceeding*, **2**, 450(2021), http://doi.org/10.5185/amp.2017/710
37. P. Liu, J. Yan, Z. Guang, Y. Huang, X. Li and W. Huang, *Journal of Power Sources*, **424**, 108(2019), http://doi.org/10.1016/j.jpowsour.2019.03.094
38. M. Naveed Ur Rehman, T. Munawar, M.S. Nadeem, F. Mukhtar, U.A. Akbar, S. Manzoor, A.S. Hakeem, M.N. Ashiq and F. Iqbal, *Solid State Sciences*, **128**, 106883(2022), http://doi.org/10.1016/j.solidstatesciences.2022.106883

[RJC-8773/2023]